

Original Article

Kras mutation subtypes distinctly affect colorectal cancer cell sensitivity to FL118, a novel inhibitor of survivin, Mcl-1, XIAP, cIAP2 and MdmX

Rabi Thangaiyan¹, Ieman AM Aljahdali^{1,2}, Kelsey Y Lent-Moore¹, Jianqun Liao^{1,3}, Xiang Ling^{1,3}, Fengzhi Li^{1,4}

¹Department of Pharmacology & Therapeutics, Roswell Park Comprehensive Cancer Center, Buffalo, New York 14263, USA; ²Department of Cellular & Molecular Biology, Roswell Park Comprehensive Cancer Center, Buffalo, New York 14263, USA; ³Canget BioTekpharma LLC, Buffalo, New York 14203, USA; ⁴Developmental Therapeutics (DT) Program, Roswell Park Comprehensive Cancer Center, Buffalo, New York 14263, USA

Received December 17, 2020; Accepted March 7, 2021; Epub July 15, 2021; Published July 30, 2021

Abstract: Mutation-activated Kras in cancer cells is a well-known challenging treatment-resistant factor that plays a critical role in treatment resistance. Human colorectal cancer (CRC) has four major Kras mutations; Kras^{G12D} (34.2%), Kras^{G12V} (21%), Kras^{G13D} (20%) and Kras^{G12C} (8.4%). Here, we report that while FL118 (a novel inhibitor of survivin, Mcl-1, XIAP, cIAP2 and MdmX) exhibits high efficacy to kill CRC cells and eliminate CRC tumors, CRC cells/tumors with different Kras mutation subtypes in the defined p53/APC genetic statuses exhibit different sensitivity to FL118 treatment. Using CRC cell lines, SW620 (Kras^{G12V}, mutant p53, mutant APC), DLD-1 (Kras^{G13D}, wild type p53, mutant APC) and SNU-C2B (Kras^{G12D}, mutant p53, wild type APC), we demonstrated that silencing of Kras^{G12V} and Kras^{G12D} using Kras-specific shRNA significantly increased CRC cell IC₅₀, while silencing of Kras^{G13D} decreased the CRC cell IC₅₀. This finding suggests that both Kras^{G12V} and Kras^{G12D} are required for showing higher FL118 efficacy, while the presence of Kras^{G13D} could somehow decrease FL118 efficacy under the defined p53/APC genetic status. Consistent with this notion, silencing of Kras^{G12V} in SW620 cells decreased FL118-induced apoptosis, while silencing of Kras^{G13D} in DLD-1 cells increased the FL118-induced apoptosis. Furthermore, forced expression of Kras^{G12V} in SW620 cells increased FL118-induced apoptosis, while forced expression of Kras^{G13D} in DLD-1 cells decreased FL118-induced apoptosis. Additionally, FL118 induced differential reactive oxygen species (ROS) production in SW620, DLD-1 and SNU-C2B cells. Our *in vivo* studies in animal models further confirmed that SW620 tumors are the most sensitive tumor to FL118 treatment; SNU-C2B tumors are the second most sensitive tumor to FL118 treatment; and the DLD-1 tumors are the least sensitive tumor. These findings would be useful for predicting FL118 sensitivity to patients' CRC tumors with the defined Kras mutation subtypes under the defined p53/APC genetic status.

Keywords: Mutant Kras, FL118, survivin, Mcl-1, XIAP, cIAP2, MdmX, colorectal cancer, human tumor animal model

Introduction

Colorectal cancer (CRC) is the second most common cause of cancer death in the United States [1]. CRC arises through the accumulation of genetic changes in key oncogenes (e.g. Kras) and tumor suppressor genes (e.g. APC, TP53) over time and is a common and heterogeneous disease [2-4]. From a therapeutic point of view, we can use the status of certain key gene mutations (e.g. Kras) as biomarkers for cancer patient stratification for personalized cancer treatment (precision medicine) if a targeted drug is available. In this regard, it is

known that mutation of Kras is involved in cancer initiation, progression, metastasis, relapse and treatment resistance. Mutant Kras is a well-known, and challenging treatment resistant factor. Development of inhibitors targeting mutant Kras is an important and active research area, although the effort to find effective mutant Kras inhibitors remains a challenge. Nevertheless, recent studies indicate that Kras mutant-specific inhibition holds promise [5]. The best demonstrated example is the Kras^{G12C} inhibitor [6]. In principle, it is possible to develop Kras^{G12D} or Kras^{G13D}-specific inhibitors through a similar Kras^{G12C} strategic

KRAS mutation subtype is a sensitivity biomarker for FL118

approach [5]. However, for some Kras mutation such as *Kras*^{G12V}, the approach used for the development of the *Kras*^{G12C} inhibitor is unlikely to be possible [5]. One potential reason for this is that *KRAS*^{G12C} is an exception, because all other mutations at residues 12, 13 and 61 decreased the affinity for the Ras-binding domain (RBD) of RAF, with an effect ranging from twofold for G12A, G13D and Q61L to sevenfold for G12V [5]. Additionally, many drugs such as the monoclonal antibody panitumumab, which targets the epidermal growth factor receptor (EGFR), needs the presence of wild type (WT) Kras for showing effective anti-metastatic CRC [7, 8]. Together, Kras mutation is a challenging issue because CRC has a high mutation rate in *Kras* (40-44.7%) [2, 9]. The major Kras mutations in CRC patients' tumors include: *Kras*^{G12D} mutations are about 34.2%; *Kras*^{G12V} mutations are about 21%; and *Kras*^{G13D} mutations are about 20%, while *KRAS*^{G12C} mutations are only about 8.4% [9]. Therefore, the inhibition of mutation-activated Kras is currently still a challenging issue in the clinic.

We have characterized a novel small molecule drug (named FL118) that shows excellent efficacy in eliminating human CRC xenograft tumors in animal models [10-12]. FL118 was identified through high throughput screening of small chemical compound libraries using the survivin gene as a biomarker and target, followed by hit-to-lead analyses [10]. FL118 is structurally similar to irinotecan and topotecan, two FDA-approved topoisomerase 1 (Top1) inhibitors used for cancer treatment in the clinic. However, FL118 can be highly efficacious to eliminate Top1-negative xenograft tumors in animal models [12], suggesting that FL118 does not require Top1 as a major therapeutic target for its antitumor activity. FL118 only weakly inhibits Top1 activity at micromolar (μM) levels; this is in sharp contrast to its strong inhibition of cancer cell growth at and below nanomolar (nM) levels [10]. Consistently, our studies show that FL118 selectively inhibits the expression of multiple downstream cancer-associated oncogenic proteins (i.e., survivin, Mcl-1, XIAP, cIAP2 and/or MdmX) in various cancer types [10, 13, 14]. It is known that irinotecan (CPT-11), SN-38 (irinotecan active metabolite), and topotecan are substrates for the efflux pump ABC transporter proteins ABCG2/BCRP [15-19] and Pgp/MDR1 [20-24]; in contrast, FL118 is not a substrate of ABCG2

[25-27] or Pgp [26-28], and can bypass treatment resistance resulting from the expression of ABCG2 and/or P-gp [25-28]. This may partially contribute to the highly effective elimination of xenograft tumors by FL118 after tumors acquired irinotecan and topotecan resistance [28]. Furthermore, while FL118 possesses superior antitumor activity, FL118 exhibits a favorable toxicity profile, with a wide therapeutic window via intravenous routes (iv) [11] or oral administration [29]. For example, the mouse maximum tolerated dose (MTD)-calculated low, middle (MTD) and high doses of FL118 in toxicity studies using beagle dogs indicated that only at the high dose, a few of the 39 hematopoietic and chemical parameters tested slightly changed without other FL118-related clinical observations including dog behavior, food consumption and body weights [29]. Furthermore, our studies also revealed that FL118 treatment of CRC cells can induce a switching of Mdm2-mediated ubiquitination and degradation of p53 (oncogenic signaling) to Mdm2-mediated ubiquitination and degradation of the oncogenic protein MdmX (apoptotic signaling), and thus, inducing CRC cell senescence and cell killing [13]. Additionally, FL118 was found to overcome the cisplatin resistance tumor cells by modulating the epithelial-to-mesenchymal transition (EMT) phenotype markers and decreasing resistance-associated proteins, ERCC1 and P-gp [30] and to inhibit-cancer stem cell markers (ABCG2, ALDH1A1, Oct4) [31].

In this study, we report that while FL118 exhibited good CRC cell killing and anti-CRC tumor activity, CRC cells and tumors with different Kras mutation subtypes exhibit different sensitivity in response to FL118 treatment in their defined p53/APC genetic status. Given that human cancer with Kras mutations is well known to be a challenging issue in the clinic, the finding reported in this study would impact on FL118 clinical application for CRC patients whose tumors have the distinct Kras gene mutation subtypes with defined p53/APC genetic statuses.

Materials and methods

Cells, cell culture and cultural reagents

CRC cell lines, SW620 (*Kras*^{G12V}, mutant p53, mutant APC), DLD-1 (*Kras*^{G13D}, wild type p53,

KRAS mutation subtype is a sensitivity biomarker for FL118

mutant APC) and SNU-C2B (Kras^{G12D}, mutant p53, wild type APC) were purchased from ATCC and cultured in the RPMI-1640 cell culture medium, which was supplemented with 10% fetal bovine serum, 100 U/ml penicillin, and 0.1 µg/mL streptomycin. Cells were cultured in a 5% CO₂ incubator at 37°C. Cells were passaged every 3-5 days with a new cell culture medium. pBabe-puro, pBabe-puro-Kras^{G12V} and pBabe-puro-Kras^{G13D} plasmids were purchased from Addgene. Kras antibodies were purchased from Cell Signaling (Beverly, MA, USA). GAPDH antibodies were purchased from Santa Cruz (Santa Cruz, CA).

FL118 drug treatment for in vitro and in vivo experiments

FL118 was synthesized in house with a purity ≥ 99%. For cell cultural studies, FL118 was first dissolved in DMSO at 1 mM and stored in aliquots at -80°C. FL118 stock solution was further diluted in DMSO to form a diluted stock solution with a dilution factor of 1000 × as final concentration with culture medium to the indicated final concentrations before use. For *in vivo* studies, the finally formulated FL118 suspension used in this study concerns FL118 (0.1-0.5 mg/mL) and hydroxypropyl-β-cyclodextrin (0.1-0.5%, w/v) in saline containing 2.5% propylene glycol (PG) and 2% hydroxypropyl methylcellulose (HPMC, 44779, Alfa Aesar). The FL118 formulation process was described in detail in the published patents [32-34]. The vehicle solution contains the corresponding concentration of hydroxypropyl-β-cyclodextrin (0.1-0.5%) in saline containing 2.5% PG and 2% HPMC without FL118. Such finally formulated FL118 suspension was orally administered weekly × 4 as its schedule.

Lentiviral shRNA infection and lentiviral particle preparation

Lentiviral vectors encoding scramble control shRNA (shC) and Kras-specific shRNA (shKras), respectively, were obtained from our Institute's shRNA Core Resource, which owns various shRNA libraries in collaboration with Open Biosystems. Lentiviral shRNA constructs packaged as pseudo-type viral particles were prepared as described in our previous studies [10]. Lentiviral particles collected from the package HEK293T cells were used to infect target CRC cells with appropriate amounts of lentiviral par-

ticles in the complete cell culture medium overnight. The medium was then replaced with a new complete cell culture medium containing 5 µg/ml puromycin (Sigma) at 48 h post-infection. A part of the puromycin resistant cells from each of the shKras1 (V2LHS_203252), shKras2 (V2LHS_169384) and shKras3 (V2LHS_202204) was used to evaluate the mutant Kras silencing using Western blots, and the rest of the pooled cells were subsequently used for the planned experiments.

Forced expression and plasmid transfection

Relevant CRC cells were transfected with pBabe-puro, pBabe-puro-KRAS^{G12V} and/or pBabe-puro-KRAS^{G13D}, respectively, using Lipofectamine 2000 transfection reagent (Invitrogen) according to the manufacturer's instructions. Stable cell clones were selected using appropriate G418 for up to 5 days. The selected cell population was used for the planned experiments.

Western blot analysis

Cells were seeded in 100 mm plates at 5 × 10⁵ cells per well. FL118 and vehicle control (DMSO) were added to the cells 24 h after plating, at 100 nM concentration. After 0-72 h of compound exposure, cells were collected and processed for total protein extraction and SDS-PAGE Western blotting was performed as previously described [35].

Cell proliferation MTT assay

Cell growth/viability was assessed using standard MTT assay described in our previous studies [36]. Briefly, Cancer cells were plated at a density of 1-2 × 10⁴ cells per well in 96-well plates and incubated overnight in a 5% CO₂ atmosphere at 37°C. The following day, cells were treated with 0-200 (or 0-500) nM FL118 concentrations prepared by serial dilutions. After 72 h of drug treatment, 20 µL MTT solution (5 mg/ml in PBS) was added to each well and incubated for 4 h at 37°C. The formed formazan crystals were dissolved in 100 µL DMSO with constant shaking. Absorbance of the solution was measured using a micro plate Reader (VersaMax, Molecular Devices) at 570 nm. The IC₅₀ value was generated from the log dose-response curves for cells using the Graphpad Prism version 9 for

KRAS mutation subtype is a sensitivity biomarker for FL118

Windows (Graphpad Software, La Jolla, CA, USA).

Apoptosis assays-Annexin V/propidium iodide (PI) staining and flow cytometry

Cell apoptosis was analyzed using Alexa Fluor 488 (or 647) Annexin V/Dead Cell Apoptosis Kit (Invitrogen, Grand Island, NY) through Annexin V-FITC/PI double staining and then quantitated by flow cytometry as previously described [10]. Briefly, CRC cells were manipulated with three conditions: (1) CRC cells were directly treated with the corresponding amount of vehicle (DMSO, control) and FL118 (100 nM), respectively; (2) CRC cells were first infected with scramble shRNA (control) and Kras-specific shRNA, respectively, to get mixed stable infectants by treating the infected cell populations with puromycin for up to 5 days and then treated with vehicle and FL118, respectively; and (3) CRC cells were first transfected with empty vectors (control) and corresponding mutant Kras expression vector, respectively, to get mixed stable transfectants by treating the transfected cell populations with G418 for up to 5 days and then treated with vehicle and FL118, respectively, for 48 h. Cells were then collected, washed with PBS, and resuspended in 1×10^6 cells/mL. Subsequently, 5 μ L Alexa Fluor 488 Annexin V and 1 μ L 100 μ g/ml PI were added to 100 μ L of the cell suspension. After 15 min incubation in the dark at room temperature, 400 μ L of $1 \times$ binding buffer were added to each tube. The resultant samples were immediately analyzed by flow cytometry. In both cases, fluorescence parameters were gated using unstained control cells and 10,000 cells were counted for each sample. The data were analyzed using WinList 3D (version 7.1) and the histogram was plotted using Excel 2010.

Analysis of reactive oxygen species (ROS)

Intracellular reactive oxygen species (ROS) were measured by two methods. One is the use of flow cytometric analysis. Briefly, after treating with FL118, cells were loaded with 20 μ M Dichloro-dihydro-fluorescein diacetate (H₂DCF-DA) (Invitrogen) and incubated at 37°C for 30 min in the dark. The samples were then immediately assayed with the FL1 channel by flow cytometry. Alternatively, ROS production from CRC cells in various conditions were analyzed

using the DCFDA/H₂DCFDA-Cellular ROS Assay Kit (ab113851, abcam). Briefly, exponentially growing DLD-1 and SNU-C2B cells were seeded (~25 K cells/well) using phenol-red complete cell culture media in a dark 96-well microplate with clear-bottom and cells were allowed to attach overnight. Next day, cells were first washed with $1 \times$ Buffer (provided in the kit) and then stained with 100 μ L of 25 μ M DCFDA in $1 \times$ Buffer for 45-55 min at 37°C in the 5% CO₂ incubator. Cells were then washed one more time with $1 \times$ Buffer before treatment with FL118 at the concentration of 10 nM and 100 nM in duplicates for 2, 4, 6, 12, 24 and 48 h with the complete cell culture medium at 37°C in the 5% CO₂ incubator. In parallel, cells treated with 50 μ M Tert-Butyl Hydrogen peroxide (TBHP) in the same time points and condition served as the positive control (provided in the kit). Fluorescence signal was detected at Ex/Em at 485/535 over time. The ROS level, proportional to fluorescence signal was normalized to ROS levels from the vehicle-treated negative control at each time point using the formula: FL118-treated ROS production fluorescence intensity divided by the corresponding vehicle-treated ROS production fluorescence intensity. Then the resultant number $\times 100\%$.

Ras pull down assay

CRC cells were treated with FL118 for 0, 12, 24, 48 and 72 h. Ras GTP levels were determined by a Ras activation assay kit (ThermoFisher Scientific) according to the manufacturer's instructions. Cell lysates (1 mg) were incubated with 10 μ g Raf-1-Ras-Binding Domain (RBD) for 45 min at 4°C on a rotating wheel and centrifuged for 15 s at 14,000 \times g to pellet agarose beads. After discarding the supernatant, agarose beads were washed three times with 500 μ L of lysis buffer and the pellets were resuspended in $2 \times$ Laemmli sample buffers containing DTT, boiled for 5 min, and centrifuged at 14,000 \times g. The pull-down Ras-GTP was subjected to separation on 12% SDS-PAGE, pulled-down KRAS was revealed by immunoblot analysis with Kras and total Ras antibodies.

Human CRC xenograft tumor animal models

The *in vivo* experimental human CRC xenograft tumor animal model studies (Animal protocol: 1192M) were approved by the Institutional

KRAS mutation subtype is a sensitivity biomarker for FL118

Animal Care and Use Committee (IACUC) at Roswell Park Comprehensive Cancer Center. All in vivo studies used female severe combined immunodeficiency (SCID) mice with an age of 8-12 weeks (body weight \geq 20 g), which were purchased from the Division of Laboratory Animal Resources (DLAR), Roswell Park Comprehensive Cancer Center. The detailed methods for the human tumor animal model studies were described in detail previously [10]. Briefly, three types of human CRC cell line-established xenograft tumor models (SW620, DLD-1, SNU-C2B) were used. These human CRC xenograft tumors were maintained on SCID mice. Experimental human CRC tumor animal models were established from the corresponding tumors isolated from the CRC tumor-maintaining SCID mice. A piece of non-necrotic tumor tissues (30-40 mg) isolated from the maintaining mice were subcutaneously transplanted on the left and/or right flank area of SCID mice. Upon the human CRC xenograft tumors were grown to 150-250 mm³ (defined as day 0 for treatment) after 7 to 14 days CRC tumor transplantation, mice were randomly divided into the planned groups (5 mice per group) for oral FL118 treatment using the weekly \times 4 schedule. Tumor length (L) and width (W) were measured using digital vernier calipers for 2-3 times per week until the end of experiments. The tumor volume (v) was calculated using the formula: $v = 0.5 (L \times W^2)$. Then the tumor size was divided by the day 0 tumor size as percentage tumor size versus day 0. The mean tumor volume \pm standard deviation (SD) at each time point was derived from 5 mice in each group. The tumor curves were made using Microsoft Excel.

Statistics analysis

Data were evaluated using the Student's t-test and GraphPad Prism version 9. $P < 0.05$ was considered as statistically significant. Data are presented as means \pm SD as indicated. For all graphs: * $P < 0.05$; ** $P < 0.01$; *** $P < 0.001$.

Results

Colorectal cancer (CRC) cells with different Kras mutation subtypes in the defined p53/APC genetic status exhibit distinct sensitivity behaviors to FL118-inhibited cell growth

Our previous limited study indicated that intraperitoneal (ip) administration of FL118 at its

maximum tolerated dose (MTD) effectively eliminates the Kras^{G12V}-mutant SW620 CRC tumors in animal models [10, 11]. Given the multiple unique features of FL118 and based on mutation-activated Kras being a well-known challenging treatment resistant factor, we thought to study whether different Kras mutation subtypes could have different behaviors to FL118 treatment in the presence and absence of mutant Kras, respectively. We first employed a lentiviral Kras shRNA (shKras) approach to silence Kras^{G12V} in SW620 and Kras^{G13D} in DLD1 CRC cells. The silencing effects of three distinct Kras shRNA (shKras, **Figure 1E**) were verified by Western Blots (**Figure 1A, 1B**). In the current study, the different three shKras-mixed pool lentiviral particles (**Figure 1E**) were used for the infection of CRC cells. We then used MTT assay to determine FL118 sensitivity in both SW620 and DLD1 cells in three distinct conditions (no infection, control scramble shRNA infection and Kras shRNA infection) treated with a series of FL118 concentrations. Then the IC₅₀ was calculated from the cell inhibition curve using SigmaPlot software. The obtained results revealed that SW620 CRC cells carrying Kras^{G12V} mutations are more sensitive to FL118 than DLD1 CRC cells carrying Kras^{G13D} mutations (0.015 nM **Figure 1C** bar 1 versus 2.31 nM **Figure 1D** bar 1). Interestingly, after silencing of Kras^{G12V} expression in SW620 cells, the sensitivity of FL118 to inhibit SW620 cell growth was significantly decreased (IC₅₀ increased from 0.017 nM to 1.19 nM, **Figure 1C** bar 2 versus bar 3). In contrast, silencing of Kras^{G13D} expression in DLD1 cells, slightly increased the sensitivity of FL118 to inhibit DLD1 cell growth (IC₅₀ decreased from 2.42 nM to 1.52 nM, **Figure 1D** bar 2 versus bar 3). This data suggests that different Kras mutation subtypes in CRC cells may differentially affect FL118 sensitivity to CRC cell growth.

CRC cells with different Kras mutation subtypes in the defined p53/APC genetic status exhibit distinct sensitivity behaviors to FL118-induced apoptosis

Next, we determined whether the differential sensitivity of SW620 cells harboring Kras^{G12V} mutation versus DLD-1 cells harboring Kras^{G13D} mutation to FL118-inhibited CRC cell growth is also accompanied with FL118-induced differential apoptosis. We performed

KRAS mutation subtype is a sensitivity biomarker for FL118

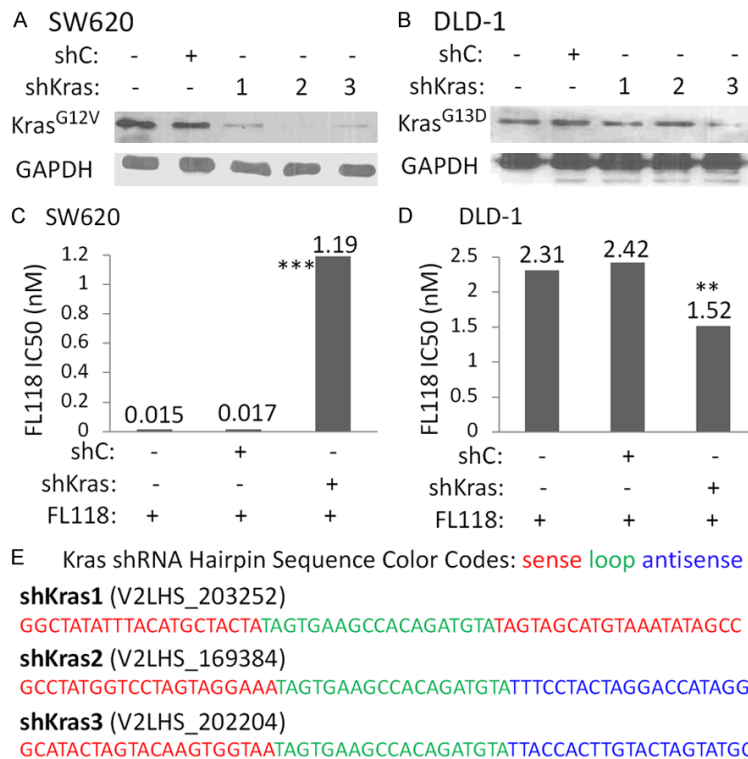


Figure 1. Silencing of *Kras* with *Kras*-specific shRNA (shKras) in colorectal cancer (CRC) cells differentially modulates FL118 sensitivity to inhibit CRC cell growth: (A, B) Validation of *Kras*^{G12V} (A) and *Kras*^{G13D} (B) silencing in SW620 (A) and DLD-1 (B) cells using Western blots. Cells were infected with lentiviral particles containing scramble control shRNA (shC, Lane 2) or shKras (Lane 3) or without infection (Lane 1), respectively. Through puromycin selection, cells were then determined for *Kras*^{G12V} and *Kras*^{G13D} expression with *Kras* antibody. GAPDH is the internal control. (C, D) CRC cells sensitivity to FL118 treatment with and without mutant *Kras* silencing. IC₅₀ in individual condition was shown. IC₅₀ calculation: SW620 (C) and DLD-1 (D) cells infected with shC (lane 2), shKras (lane 3) lentiviral particles or without infection (lane 1) were seeded in 96 well plates overnight, respectively. Cells were then treated with a series of FL118 concentrations in triplicates for 3 days, followed by MTT assays to determine cell growth and viability curves. FL118 IC₅₀ values were then calculated from the comprehensive MTT data. (E) The DNA sequence information of the five individual *Kras* shRNA in lentiviral vectors was shown.

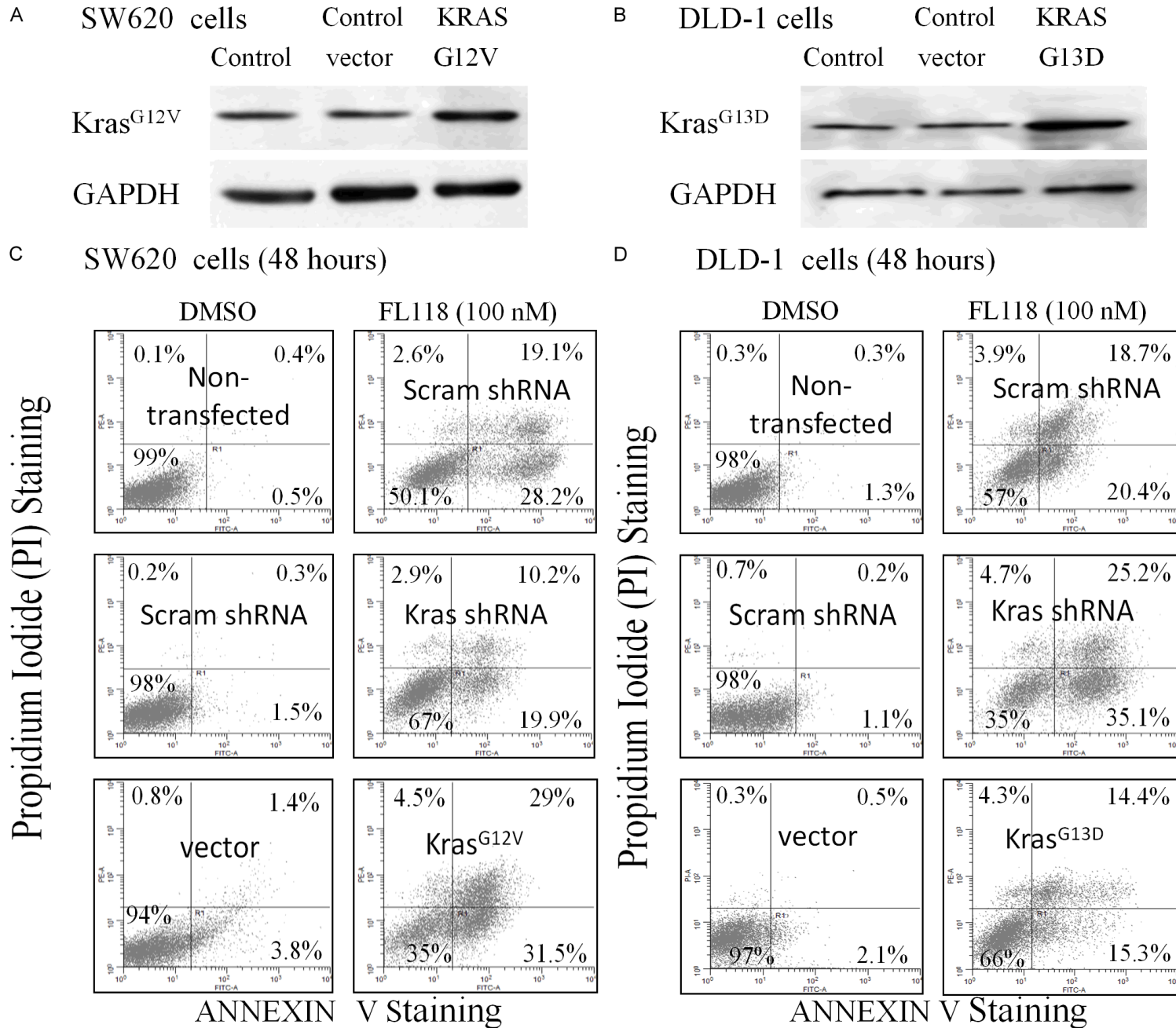
Annexin V-FITC/PI flow cytometry to determine CRC cell apoptosis in the situations of (1) SW620 or DLD-1 cells without transfection treated with DMSO vehicle (**Figure 2C, 2D**, top panel left); (2) SW620 or DLD-1 cells transfected Scram shRNA and treated with DMSO and FL118, respectively (**Figure 2C, 2D**, top panel right and middle panel left); (3) SW620 or DLD-1 cells transfected *Kras* shRNA and treated with FL118 (**Figure 2C, 2D**, middle panel right); and (4) SW620 or DLD-1 cells with exogenously overexpressed vector or mutant *Kras* treated with DMSO or FL118, respectively (**Figure 2C, 2D**, bottom panel) as shown. A part

of these cells was used to validate the forced expression status of mutant *Kras* as shown in **Figure 2A** (SW620 cells) and **Figure 2B** (DLD-1 cells). Annexin V and PI staining followed by flow cytometry analysis revealed that silencing of *Kras*^{G12V} using *Kras* shRNA decreases FL118 relative ability to induce apoptosis, while overexpression of *Kras*^{G12V} increases the relative ability of FL118 to induce apoptosis (**Figure 2C**). In contrast, silencing of *Kras*^{G13D} using *Kras* shRNA increased FL118 relative ability to induce apoptosis, while overexpression of *Kras*^{G13D} decreased the relative ability of FL118 to induce apoptosis (**Figure 2D**). These results revealed the same concept that CRC cells with different *Kras* mutation subtypes in the defined p53/APC genetic status could differentially respond to FL118 treatment.

FL118 took advantage of mutation-activated Kras-mediated production of reactive oxygen species (ROS) to kill CRC cells as an additional mechanism

Next, we studied the role of mutant *Kras* in FL118-induced CRC cell ROS production and cell killing. It has been reported that *Kras*^{G12V} (K-ras V12) predominantly signals through activation of the p38/PDPK1/PKCδ/p47^{phox}/NOX1 cascade and promotes ROS formation in CRC cells [37]. In this regard, we found that FL118 appears to take advantage of the activated *Kras*-mediated ROS formation pathway to increase ROS production to kill cancer cells, which appears to be an early onset event (see **Figure 4** below). Specifically, in the presence of *Kras*^{G12V} mutation, FL118 treatment strikingly increases ROS production in CRC cells (**Figure 3A** upper panel). In contrast, silencing of *Kras*^{G12V} in CRC cells significantly diminished ROS production induced by

KRAS mutation subtype is a sensitivity biomarker for FL118



KRAS mutation subtype is a sensitivity biomarker for FL118

Figure 2. CRC cells with different *Kras* mutation subtypes exhibited differential sensitivity to FL118-induced apoptosis: (A, B) Validation of *Kras*^{G12V} (A) and *Kras*^{G13D} (B) overexpression in SW620 (A) and DLD-1 (B) cells, respectively. Cells were transfected with control expression vector (Control vector, Lane 2) or corresponding mutant *Kras* expression vectors (Lane 3) or without transfection (Lane 1), respectively. Through G418 selection, cells were then determined for *Kras*^{G12V} and *Kras*^{G13D} expression with *Kras* antibody, respectively. GAPDH is the internal control. (C) FL118 affects apoptosis of SW620 cells with *Kras*^{G12V} mutation in the defined p53/APC genetic status. SW620 cells without infection (top panel left) or infected with lentiviral scramble shRNA (Scram shRNA, top panel right and middle panel left) and *Kras*-specific shRNA (*Kras* shRNA, middle panel right), respectively. Alternatively, SW620 cells were transfected with empty vector (bottom panel left) and *Kras*^{G12V} expression vector (bottom panel right) respectively. After selection with puromycin (top panel right and middle panel) or with G418 (bottom panel), cells were treated with vehicle (DMSO control, left panel) and FL118 for 48 h (right panel), respectively, as shown. Cells with and without FL118 treatment were undergoing the process of Annexin V and PI staining, followed by flow cytometry analysis. Results from an example experiment are shown. (D) FL118 affects apoptosis of DLD-1 cells with *Kras*^{G13D} mutation in the defined p53/APC genetic status. DLD-1 cells without infection (top panel left) or infected with lentiviral Scram shRNA (top panel right and middle panel left) and *Kras* shRNA (middle panel right), respectively. Alternatively, DLD-1 cells were transfected with empty vector (bottom panel left) or transfected with *Kras*^{G13D} expression vector (bottom panel right) respectively. After selection with puromycin (top panel right and middle panel) or with G418 (bottom panel), cells were treated with vehicle (DMSO control, left panel) and FL118 for 48 h (right panel), respectively, as shown. DLD-1 cells with and without FL118 treatment were undergoing the process of Annexin V and PI staining, followed by flow cytometry analysis. Results from an example experiment are shown. Of note, cells transfected with *Kras* shRNA without FL118 treatment is about 5% apoptosis and cells transfected with *Kras*^{G12V} expression vector treated with DMSO is similar to non-transfected cells treated with DMSO. For simplifying the presentation, these controls were omitted.

FL118 treatment (**Figure 3A** lower panel). This observation suggests that FL118-mediated production of ROS is *Kras*^{G12V} status-dependent. Consistent with this observation, our Ras-GTP pull-down assay revealed that treatment of SW620 cells with FL118 does not inhibit Ras-GTP activity over time (**Figure 3B**). Next, we determined whether the *Kras*^{G12V} status-dependent production of ROS stimulated by FL118 treatment (**Figure 3A**) is accompanied by apoptosis induction in CRC cells and whether the apoptosis is also *Kras*^{G12V} status-dependent. Our study revealed that silencing of *Kras*^{G12V} significantly diminishes apoptosis determined by Annexin V staining, while forced expression of *Kras*^{G12V} significantly increases apoptosis (**Figure 3C**). Importantly, in the presence of the ROS scavenger/inhibitor N-acetyl-L-cysteine (NAC, 10 mM), the apoptosis level was significantly diminished upon FL118 treatment (**Figure 3C**), suggesting that the increased ROS production is at least partially involved in FL118-mediated apoptosis induction (see our discussion in the “Discussion” section).

In order to confirm that the FL118-induced ROS production is an early onset strategy for FL118 to kill CRC cells, we performed a more detailed time course of FL118 treatment in DLD-1 and SNU-C2B CRC cells for up to 48 h. As shown in **Figure 4**, similar to the case in SW620 cells (i.e., FL118 promoted ROS production to kill

CRC cells, **Figure 3**), after FL118 treatment of DLD-1 or SNU-C2B cells, ROS production was significantly increased as short as with 2 h FL118 treatment, and ROS reached a peak production at 4 h (**Figure 4**). Interestingly, after 24 h and 48 h treatment, ROS production from CRC cells came back to the vehicle control level or close to the vehicle control (**Figure 4**). This result confirmed that promotion of ROS production by FL118 treatment is an early event for FL118 to kill CRC cells. This finding is in contrast to the previous finding that FL118-induced inhibition of survivin, Mcl-1, XIAP and cIAP2 is a sustained event [10, 38, 39]. Thus, in addition to the mechanisms found in our previous studies, FL118-induced ROS production would be an additional mechanism for FL118 to kill cancer cells.

*Distinct antitumor activity of FL118 on CRC tumors possessing different *Kras* mutation subtypes in the defined p53/APC genetic status*

SW620 cells have the *Kras*^{G12V} mutation, while DLD-1 cells have the *Kras*^{G13D} mutation. Based on our finding presented in **Figures 1-4**, we expect that while both cell line-established xenograft tumors could be sensitive to FL118 treatment, SW620 xenograft tumors should be more sensitive than DLD-1 xenograft tumors to FL118 treatment. Consistent with this expectation, we found that (1) SW620 tumors are highly sensitive to FL118 treatment and can

KRAS mutation subtype is a sensitivity biomarker for FL118

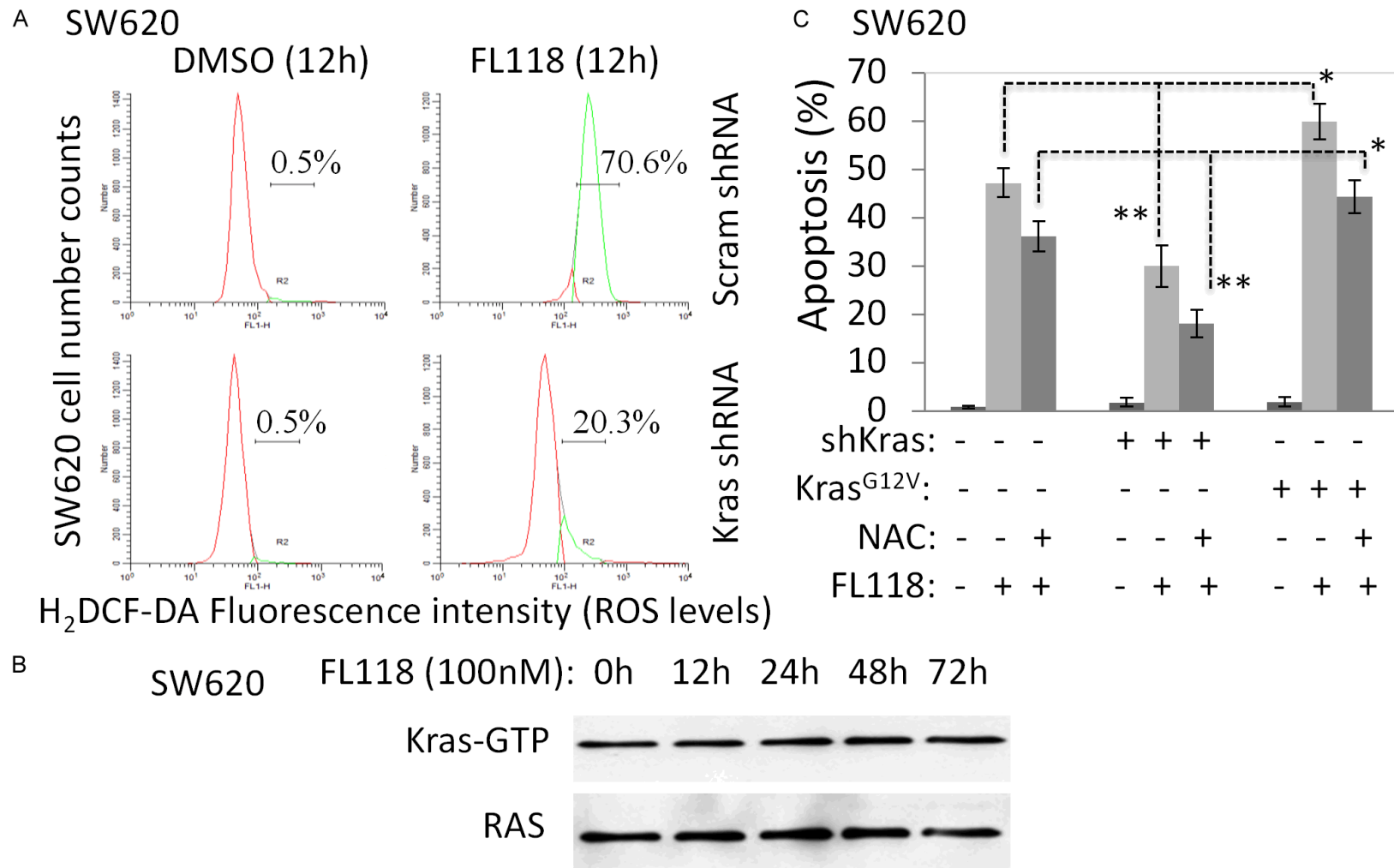


Figure 3. Kras-mediated ROS production plays an important role in FL118-induced apoptosis in SW620 cells: A. SW620 cells were genetically manipulated as shown. The intracellular ROS were measured via flow cytometry. Briefly, after treating with and without FL118 (100 nM) for 12 h, the genetically manipulated SW620 cells were loaded with 20 μ M Dichloro-dihydro-fluorescein diacetate (H₂DCF-DA) and incubated at 37 °C for 30 min in the dark. The samples were then immediately determined for ROS production using flow cytometry. A typical example result is shown. Y axis is the setting internal control-normalized cell counts and X axis is the ROS production level reflected by H₂DCF-DA-released fluorescence intensity. B. FL118 effects on Ras-GTP activity. Ras-GTP pull-down assay was performed as described in the Materials and Methods to determine the effect of FL118 on Ras-GTP activity over time. C. The genetically engineered SW620 cells as shown were treated with and without FL118 at 100 nM in the presence and absence of the ROS inhibitor N-acetyl-L-cysteine (NAC, 10 mM) for 72 h. Apoptotic cells were determined by Annexin V labeling. The data are the mean \pm SD derived from two independent experiments.

KRAS mutation subtype is a sensitivity biomarker for FL118

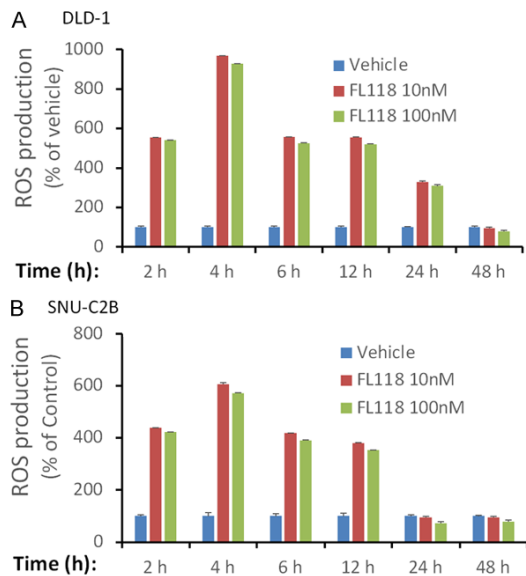


Figure 4. FL118-induced ROS production in DLD-1 and SNU-C2B CRC cells: ROS production in CRC cells were determined using the DCFDA/H2DCFDA-Cellular ROS Assay Kit (ab113851, Abcam) through measuring the fluorescence intensity in the black 96-well plate with clear-bottom. The detailed procedure is described in the “Materials and Methods” section. A. ROS production in DLD-1 cells after treatment with vehicle (DMSO, control) and FL118 (10, 100 nM), respectively, over a time course of 2 h, 4 h, 6 h, 12 h, 24 h and 48 h. B. ROS production in SNU-C2B cells after treatment with vehicle (DMSO, control) and FL118 (10, 100 nM), respectively, over a time course of 2 h, 4 h, 6 h, 12 h, 24 h and 48 h. The data are the mean \pm SD derived from two independent experiments.

eliminate tumor under FL118 MTD. Specifically, FL118 could eliminate tumor at 10 mg/kg (MTD), 5 mg/kg and 3.75 mg/kg (Figure 5A), while exhibiting only a temporary animal body weight loss within 20% at the FL118 MTD level (Figure 5B). This suggests no serious FL118-induced toxicity in animals; and (2) DLD-1 xenograft tumor is indeed much less sensitive to FL118 treatment even at the FL118 MTD (10 mg/kg) and with the same schedule of weekly \times 4 times for oral administration (Figure 5C). This is consistent with the finding shown in Figure 1.

In order to confirm the concept that CRC xenograft tumors with distinct Kras mutation subtypes have differential sensitivity to FL118 treatment, we further used the SNU-C2B CRC cells and SNU-C2B cell-established xenograft tumors to alternatively perform *in vitro* and *in*

in vivo studies. In contrast to the SW620 cells having the Kras^{G12V} mutation, and DLD-1 cells having the Kras^{G13D} mutation, the SNU-C2B cells have the Kras^{G12D} mutation. Intriguingly, our *in vitro* studies revealed that similar to the case of SW620 (Figure 1A, 1C), silencing of Kras^{G12D} expression in SNU-C2B cells increased FL118 IC₅₀ from 0.82 nM to 3.6 nM (Figure 6A, 6C). However, forced expression of Kras^{G12D} in SNU-C2B cells did not change the IC₅₀ of FL118 to inhibit the SNU-C2B cell growth (Figure 6B, 6D). These findings made us expect that SNU-C2B cell-established xenograft tumors should be less sensitive to FL118 treatment than SW620 tumors but should be more sensitive to FL118 treatment than DLD-1 xenograft tumors. Consistent with this expectation, the SNU-C2B-derived xenograft tumor indeed exhibited less sensitivity to FL118 treatment than SW620-established tumors, while exhibiting more sensitivity to FL118 treatment than DLD-1-established xenograft tumors (compare Figure 6E to Figure 5 and 5C).

In order to further confirm the overall conclusion derived from both *in vitro* molecular level studies and *in vivo* CRC tumor animal model studies (Figures 1-6), we alternatively re-performed the three CRC cell lines (SW620, DLD-1, SNU-C2B) for growth inhibition by FL118 to determine their sensitivity to FL118-induced growth inhibition. The data derived from this straightforward experiment is consistent with other data shown in our other studies (Figures 1-6). That is, SW620 is more sensitive to FL118 treatment than DLD-1 and SNU-C2B cells (Figure 7).

Discussion

Kras mutation in cancer is a serious issue, especially in CRC and pancreatic ductal adenocarcinoma (PDAC) tumors (see below). Our recent studies demonstrated that bladder cancer cells with mutant Kras (mKras) are more sensitive to FL118 treatment in comparison with bladder cancer cells with wild type Kras [39]. In this study, we demonstrated that while FL118 exhibited excellent anti-CRC activity for CRC cells and CRC tumors with different Kras mutation subtypes, CRC tumors with different Kras mutation subtypes in the defined p53/APC genetic status exhibited distinct sensitivity behaviors in response to FL118 treatment.

KRAS mutation subtype is a sensitivity biomarker for FL118

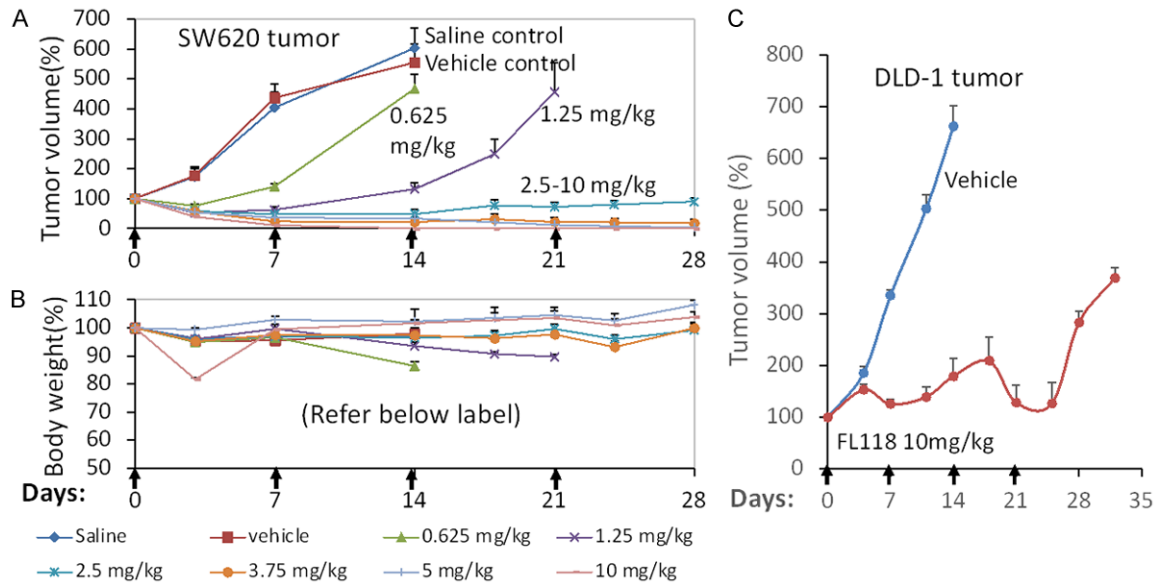


Figure 5. Antitumor activity of FL118 for CRC SW620 ($Kras^{G12V}$) and DLD-1 ($Kras^{G13D}$)-established tumors: (A) Anti-tumor curves of SW620-derived xenograft tumors after FL118 treatment. Establishment of xenografts from cancer cells were described in our previous study [10]. Establishment of human tumor mouse models: Experimental Severe combined immunodeficiency (SCID) mice were subcutaneously implanted with SW620 tumors at the left or right flank area of the SCID mice. Treatment was initiated 7 days after subcutaneous tumor implantation (designated day 0), at which tumor size was about 100-200 mm³. FL118 was orally administered from day 0 at MTD (10 mg/kg) and sub-MTD doses in a weekly \times 4 schedule as shown (arrowed). Each curve is the mean \pm SD derived from five individual tumors (5 mice per group). (B) Mouse body weight change curves. Each curve is the mean \pm SD derived from five individual body weights (5 mice per group) to reflect the potential toxicity of FL118. Individual color curve labeling is put at the bottom (A, B). (C) Antitumor curves of DLD-1-derived xenograft tumors after FL118 treatment. Experimental human tumor mouse model establishment is the same as described in (A). Treatment was initiated 7-14 days after subcutaneous tumor implantation, which depended on tumor growing size (designated day 0), at which tumor size was about 100-200 mm³. FL118 was orally administered from day 0 at 10 mg/kg (MTD) in a weekly \times 4 schedule as shown (arrowed). Each curve is the mean \pm SD derived from five individual tumors (5 mice per group).

Specifically, we found that after the silencing of $Kras^{G12V}$ in SW620 cells ($Kras^{G12V}$, mutant p53, mutant APC) and $Kras^{G12D}$ in SNU-C2B cells ($Kras^{G12D}$, mutant p53, wild type APC) using $Kras$ -specific shRNA, these mutant $Kras$ -silenced SW620 cells or SNU-C2B cells increased FL118 IC₅₀ (Figures 1A, 1B, 6A and 6B; i.e., decrease sensitivity to FL118). This observation suggests that such $Kras$ mutation subtypes ($Kras^{G12V}$, $Kras^{G12D}$) in the defined p53/APC genetic status are required to maintain higher sensitivity of CRC cells to FL118 treatment. In contrast, when we silenced $Kras^{G13D}$ in DLD-1 cells ($Kras^{G13D}$, wild type p53, mutant APC) using $Kras$ -specific shRNA, we found that the $Kras^{G13D}$ subtype-silencing cells decreased FL118 IC₅₀ (Figure 1B, 1D). This observation suggests that the presence of the $Kras^{G13D}$ subtype mutation in the defined p53/APC genetic status somehow decreases the sensitivity of DLD-1 CRC cells to FL118 treat-

ment. Consistently, SW620 cells with the silenced $Kras^{G12V}$ mutation subtype in the defined p53/APC genetic status showed decreased FL118-induced apoptosis (Figure 2C, middle panel). In contrast, DLD-1 cells with the silenced $Kras^{G13D}$ mutation subtype in the defined p53/APC genetic status showed increased FL118-induced apoptosis (Figure 2D, middle panel). Alternative studies obtained the same notion. Specifically, after we overexpressed $Kras^{G12V}$ in SW620 cells, such $Kras^{G12V}$ -overexpressed SW620 cells increased FL118-induced apoptosis (Figure 2C, bottom panel). In contrast, after we overexpressed $Kras^{G13D}$ in DLD-1 cells, such $Kras^{G13D}$ -overexpressed DLD-1 cells decreased FL118-induced apoptosis (Figure 2D, bottom panel). Here we would like to emphasize that while our data clearly suggested that different $Kras$ mutation subtypes exhibited distinct sensitivity to FL118 treatment, the defined p53/APC genetic status

KRAS mutation subtype is a sensitivity biomarker for FL118

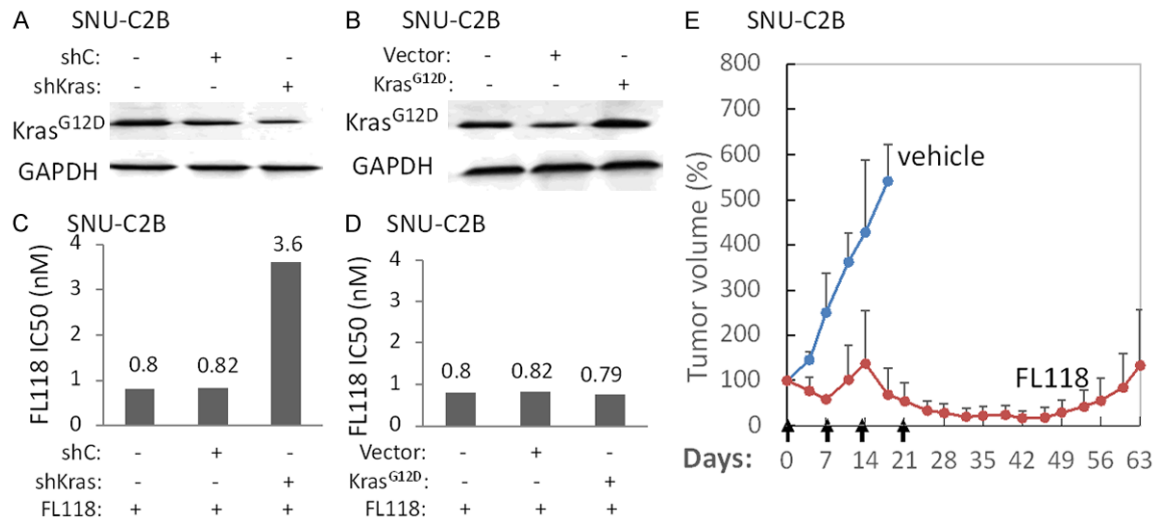


Figure 6. Antitumor activity of FL118 in CRC Kras^{G12D} SNU-C2B cells (*in vitro*) and the cell-established tumors (*in vivo*): (A) Validation of Kras^{G12D} silencing in SNU-C2B using Western blots. A part of the SNU-C2B cells without lentiviral particle infection, with control scramble shRNA (shC) and with Kras-specific shRNA lentiviral particles (shKras), respectively, as shown were processed by Western blots. (B) Validation of the forced expression of Kras^{G12D} using Western blots. A part of the SNU-C2B cells without transfection, with control expression vector transfection (vector) and with Kras^{G12D} expression vector transfection, respectively, as shown were analyzed with Western blots. GAPDH in (A and B) is the internal control. (C) The other part of the SNU-C2B cells manipulated as described in (A) were seeded in 96-well plates overnight, and then treated with a series of FL118 concentrations in triplicates for 3 days, followed by MTT assays to determine cell growth/viability curves. FL118 IC₅₀ values were then calculated from the MTT data and presented in (C). (D) The other part of the SNU-C2B cells manipulated as described in (B) were seeded in 96-well plates overnight, and then treated with a series of FL118 concentrations in triplicates for 3 days, followed by MTT assays to determine cell growth/viability curves. FL118 IC₅₀ values were then calculated from the MTT data and presented in (D). (E) Antitumor potential of FL118 in SNU-C2B-established xenografts: Tumor models were set up as in the Figure 5A legend. FL118 was orally administered via weekly × 4 (arrows) at a dose of 10 mg/kg (MTD) in the defined formulation. The tumor growth curve over time is the mean ± SD derived from five mice.

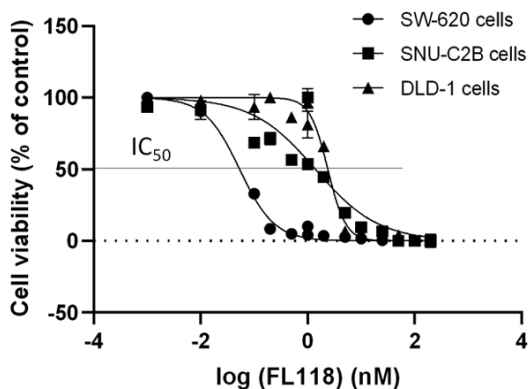


Figure 7. Sensitivity of the CRC cell lines, SW620, DLD-1 and SNU-C2B to FL118 treatment in terms of cell growth inhibition. Subconfluent SW620 cells, DLD-1 cells and SNU-C2B cells in 96-well plates were treated with and without FL118 in a series of concentrations for 72 h as shown. Cell growth was then analyzed using MTT assay. The data is the mean derived from 3 independent MTT determinations plotted in log scale.

may also affect the corresponding Kras mutation subtypes and thus affect the correspond-

ing CRC cell line sensitivity to FL118 treatment, especially in the case of TP53/p53 genetic status (see the next paragraph below for more information). This possibility could not be ruled out in our studies since the three CRC cell lines that were used have distinct p53/APC genetic status.

Here we would like to emphasize that the underlying molecular mechanism for CRC cells with the distinct Kras gene status (i.e., different mutation subtypes or wild type) that shows distinct sensitivity to FL118 treatment needs further investigation. However, the status of the differential three key gene/protein mutation status in CRC cells (Kras, TP53/p53, APC) may provide a partial explanation. That is, SW620 cells have Kras^{G12V} together with double p53 and APC mutations; SNU-C2B CRC cells have Kras^{G12D} together with mutant p53 and wild type APC; and DLD-1 cells have Kras^{G13V} together with wild type p53 and mutant APC. Whether the mutant or wild type status of p53 and APC may affect CRC cells with distinct Kras

KRAS mutation subtype is a sensitivity biomarker for FL118

mutation subtypes would need further investigation, our previous studies indicate that CRC cells without a functional p53 are more sensitive to FL118 treatment than CRC cells with wild-type p53 (wtp53) [13]. A recent research article published in *Nature* demonstrated that loss of a functional p53 increases mutant Kras dosage acquisition [40]. In this regard, loss of functional p53 can result from point mutation, microdeletion or homocopolymer [41], which is collectively called mutant p53. Significantly, consistent with the finding that loss of functional p53 increases mutant Kras dosage acquisition in PDAC [40], Kras mutation is associated with p53 mutation in PDAC [42, 43]; and mutant Kras and mutant p53 can cooperate in the establishment of PDAC [42]. Although mutant Kras and mutant p53 are not as closely associated in CRC as they are in PDAC, mutation-activated oncogenic Kras is shown to be a driver of CRC invasion and metastases [44], and the multiple combination approach is an effective way to reverse mutant Kras-mediated apoptosis resistance [45]. Furthermore, most if not all the current available anti-cancer drugs exhibit better antitumor efficacy if tumors show no mutations in Kras and p53. For example, it was shown that lack of mutations in Kras, Nras, Braf and p53 (*TP53*) improves the outcome of elderly metastatic CRC patients treated with cetuximab, oxaliplatin and uracil/ftorafur [46]. In this regard, FL118 may fill in an unmet need and specifically target tumors with mutations in both Kras and p53 genes. Nevertheless, studies of mutant Kras and mutant p53 relationship may provide some explanation for the finding reported in this study. Given that the mutation rate of p53 in CRC is at a range of 60-70% [2] and in PDAC is at a range of 50-70% [41-43], while the mutation rate of Kras in CRC is at a range of 40-44.7% [2, 9] and in PDAC is at a range of 70-90% [42, 43], the findings reported in this study would be useful for predicting FL118 sensitivity to patients' CRC tumors with the defined Kras mutation subtype status together with the genetic status of TP53/p53 (mutant versus wild type). Additionally, as we mentioned in the "Introduction" section, there are four major types of Kras mutation: *Kras*^{G12D} mutations (~34.2%), *Kras*^{G12V} mutations (~21%), *Kras*^{G13D} mutations (~20%), and *KRAS*^{G12C} mutations (~8.4%) [9]. Our studies in this report have covered the first 3 types. In

turn, the sensitivity of CRC tumor with *KRAS*^{G12C} mutation to FL118 treatment would be a valuable thing to know. In this regard, the CRC cell line SW1463 has the *Kras*^{G12C} mutation with p53/APC double mutations. Our previous studies indicated that at the dose of FL118 MTD, FL118 showed similar or little less sensitive efficacy in SW1463-established tumors [12] in comparison with the SNU-C2B tumor data shown in this study (**Figure 6E**).

While the findings discussed above are intriguing and lay a basis for further investigation, the underlying mechanism by which CRC cells with different Kras mutation subtypes exhibited distinct sensitivity behaviors in response to FL118 treatment may involve additional mechanisms and require further investigation. In this regard, our limited studies indicated that the induction of reactive oxygen species (ROS) production by FL118 treatment among the three CRC cell types may only partially explain the finding. In other words, while SW620 cells exhibited the highest ROS production upon FL118 treatment, DLD-1 cells produce more ROS than those produced by SNU-C2B cells after FL118 treatment. For example, at the 12 h time point, after FL118 (100 nM) treatment, SW620 cells increased 140-fold ROS production (70.6% divided by 0.5%, **Figure 3A**, upper panel); DLD-1 cells increased about 5-fold ROS production (~500% divided by 100%, **Figure 4A**) and SNU-C2B cells increased less than 4-fold ROS production (387% divided by 100%, **Figure 4B**), although the difference of ROS production in DLD-1 and SNU-C2B CRC cells are very similar after FL118 treatment. This is consistent with our previous studies indicating that FL118-mediated inhibition of survivin, Mcl-1, XIAP, cIAP2 and MdmX is involved in FL118 function in terms of inhibition of cancer cell growth and induction of cancer cell apoptosis [10, 13, 38, 39]. Together, FL118-induced rapid ROS production is likely involved in early FL118 function as an additional mechanism for FL118 to kill cancer cells in addition to the mechanisms through the inhibition of survivin, Mcl-1, XIAP, cIAP2 and MdmX. Nevertheless, several studies revealed that ROS plays an important role in the Kras-induced malignant transformation [37]. It was well characterized that oncogenic *Kras*^{G12V} induces activation of p38/PDPK1/PKC δ /p47^{phox}/NOX1-dependent ROS generation [37].

Therefore, we propose that FL118-induced ROS overproduction at least partially plays a role in CRC cells' differential sensitivity to FL118-induced cell killing. Nevertheless, one thing that is certain in our FL118-induced ROS production studies is that FL118-induced ROS production is an early event. This is clearly indicated in the data shown in **Figure 4** for the dynamic ROS production over time after FL118 treatment. This finding is in contrast to the inhibition of survivin, Mcl-1, XIAP and/or cIAP2 by FL118, which is relatively permanent as a sustained event [10, 38, 39]. Nevertheless, our *in vivo* studies in animal models also indicated that SW620-established xenograft tumors are the most sensitive tumor to FL118 treatment; SNU-C2B tumors are the second most sensitive tumor to FL118 treatment; and DLD-1 tumors are the least sensitive tumor among the three CRC tumors with distinct Kras mutation subtypes.

One intriguing question is whether ROS production induced by FL118 could affect the activation/expression of survivin, Mcl-1, XIAP, cIAP2 and MdmX. To answer this intriguing question, while we do not know whether ROS can influence the activation/expression of survivin, Mcl-1, XIAP, cIAP2 and MdmX, what we indeed know is that (1) FL118 can rapidly induce ROS production after a 2 h FL118 treatment and reach a peak of ROS production in a 4 h FL118 treatment, gradually decreasing over time (**Figure 4**); and (2) FL118-induced inhibition of survivin, Mcl-1, XIAP, cIAP2 and MdmX employs both transcriptional and non-transcriptional mechanisms. This is cancer type-dependent and for a defined cancer cell type, it can employ one mechanism or another, or employ both mechanisms. Downregulation of survivin, Mcl-1, XIAP, cIAP2 and MdmX by FL118 can be as short as 8 hours (via a non-transcriptional mechanism) and be as long as a minimum time of 16-24 h (transcriptional mechanism). Therefore, if ROS production can have any effects on the expression/activation of survivin, Mcl-1, XIAP, cIAP2 and MdmX, a logical expectation should be a negative effect (i.e., ROS inhibition of the expression/activation of survivin, Mcl-1, XIAP, cIAP2 and MdmX). This expectation is consistent with the previously reported studies which revealed that apoptosis induced by sulindac and arsenic trioxide in human lung cancer A549 cells is through ROS-dependent down-regulation of survivin [47].

Finally, the finding in this report was further alternatively confirmed through using the three CRC cell line (SW620, DLD-1 and SNU-C2B) to re-determine their sensitivity to FL118-induced growth inhibition. The data shown in **Figure 7** is consistent with the conclusion derived from the *in vitro* molecule level studies and the *in vivo* CRC tumor animal model studies (**Figures 1-6**). Based on this observation, we would like to emphasize that we have re-performed a simple experiment for the data presented in **Figure 7**, instead of using a complex experiment through first silencing a corresponding Kras mutation subtype and then forcing expression of it again by transfection/infection. This is based on several considerations: (1) we have performed both silencing and overexpression of Kras mutation subtype, respectively, in our studies and obtained a clear conclusion. These are simple genetic manipulations and thus the experimental outcome is more reliable than complex genetic manipulation-based outcomes; (2) it is known that transfection/infection efficiency could not reach 100% and thus many cells would only have one genetic manipulation with or without selection; and (3) any cells with two genetic manipulation processes will have the interference of those two genetic manipulations, and as a result, the follow-up forced overexpression of a gene will not be effective and may be continuously inhibited by the first silencing process, or the endogenous gene would serve the same role. When possible, use of the natural cell to perform an experiment would help to preclude potential issues occurring from the complex genetic manipulation of cancer cells.

In conclusion, in this study, by using multiple *in vitro* and *in vivo* approaches we demonstrated that CRC cells/tumors with different Kras mutation subtypes under the defined p53/APC genetic status exhibited distinct sensitivity to FL118 treatment. This is critical for cancer patient selection and predicting tumor sensitivity to FL118 treatment during clinical trials.

Acknowledgements

This research work was sponsored in part by NIH Grants, R21CA180764, R03CA182552, R44CA176937 and P30CA016056 (NCI Cancer Center Core Support Grant) as well as the 2020 Pancreatic Cancer Action Network (PanCAN) Translational Research Grant (20-65-FENG).

The authors would like to thank Ms. Amanda Hess for the editorial check of this manuscript before submission.

Disclosure of conflict of interest

FL118 and FL118 core structure-based analogues will be further developed in Canget BioTekpharma LLC (www.canget-biotek.com), a Roswell Park Cancer Institute-spinoff company. FL, XL are initial investors of Canget for development of FL118 and FL118 core structure-relevant anticancer agents and own Canget equity.

Address correspondence to: Drs. Fengzhi Li and Xiang Ling, Department of Pharmacology & Therapeutics, Roswell Park Comprehensive Cancer Center, Elm and Carlton Streets, Buffalo, New York 14263, USA. Tel: 716-845-4398; Fax: 716-845-8857; E-mail: fengzhi.li@roswellpark.org (FZL); Xiang.Ling@RoswellPark.org (XL)

References

- [1] Siegel RL, Miller KD, Goding Sauer A, Fedewa SA, Butterly LF, Anderson JC, Cercek A, Smith RA and Jemal A. Colorectal cancer statistics, 2020. *CA Cancer J Clin* 2020; 70: 145-164.
- [2] Fearon ER. Molecular genetics of colorectal cancer. *Annu Rev Pathol* 2011; 6: 479-507.
- [3] Ewing I, Hurley JJ, Josephides E and Millar A. The molecular genetics of colorectal cancer. *Frontline Gastroenterol* 2014; 5: 26-30.
- [4] Tomlinson I, Ilyas M and Novelli M. Molecular genetics of colon cancer. *Cancer Metastasis Rev* 1997; 16: 67-79.
- [5] Ostrem JM and Shokat KM. Direct small-molecule inhibitors of KRAS: from structural insights to mechanism-based design. *Nat Rev Drug Discov* 2016; 15: 771-785.
- [6] Hobbs GA, Wittinghofer A and Der CJ. Selective targeting of the KRAS G12C mutant: kicking KRAS when it's down. *Cancer Cell* 2016; 29: 251-253.
- [7] Amado RG, Wolf M, Peeters M, Van Cutsem E, Siena S, Freeman DJ, Juan T, Sikorski R, Suggs S, Radinsky R, Patterson SD and Chang DD. Wild-type KRAS is required for panitumumab efficacy in patients with metastatic colorectal cancer. *J Clin Oncol* 2008; 26: 1626-1634.
- [8] Pietrantonio F, Perrone F, Biondani P, Maggi C, Lampis A, Bertan C, Venturini F, Tondulli L, Ferrari D, Ricci V, Villa F, Barone G, Bianco N, Ghidini A, Bossi I, Fanetti G, Di Bartolomeo M and de Braud F. Single agent panitumumab in KRAS wild-type metastatic colorectal cancer patients following cetuximab-based regimens: clinical outcome and biomarkers of efficacy. *Cancer Biol Ther* 2013; 14: 1098-1103.
- [9] Cox AD, Fesik SW, Kimmelman AC, Luo J and Der CJ. Drugging the undruggable RAS: mission possible? *Nat Rev Drug Discov* 2014; 13: 828-851.
- [10] Ling X, Cao S, Cheng Q, Keefe JT, Rustum YM and Li F. A novel small molecule FL118 that selectively inhibits survivin, Mcl-1, XIAP and cIAP2 in a p53-independent manner, shows superior antitumor activity. *PLoS One* 2012; 7: e45571.
- [11] Ling X and Li F. An intravenous (i.v.) route-compatible formulation of FL118, a survivin, Mcl-1, XIAP, and cIAP2 selective inhibitor, improves FL118 antitumor efficacy and therapeutic index (TI). *Am J Transl Res* 2013; 5: 139-154.
- [12] Li F, Ling X, Harris DL, Liao J, Wang Y, Westover D, Jiang G, Xu B, Boland PM and Jin C. Topoisomerase I (Top1): a major target of FL118 for its antitumor efficacy or mainly involved in its side effects of hematopoietic toxicity? *Am J Cancer Res* 2017; 7: 370-382.
- [13] Ling X, Xu C, Fan C, Zhong K, Li F and Wang X. FL118 induces p53-dependent senescence in colorectal cancer cells by promoting degradation of MdmX. *Cancer Res* 2014; 74: 7487-7497.
- [14] Holthof LC, van der Horst HJ, van Hal-van Veen SE, Ruiter RWJ, Li F, Buijze M, Andersen MN, Yuan H, de Bruijn J, van de Donk NWCJ, Lokhorst HM, Zweegman S, Groen RWJ and Mutis T. Preclinical evidence for an effective therapeutic activity of FL118, a novel survivin inhibitor, in patients with relapsed/refractory multiple myeloma. *Haematologica* 2020; 105: e80-e83.
- [15] Houghton PJ, Germain GS, Harwood FC, Schuetz JD, Stewart CF, Buchdunger E and Traxler P. Imatinib mesylate is a potent inhibitor of the ABCG2 (BCRP) transporter and reverses resistance to topotecan and SN-38 in vitro. *Cancer Res* 2004; 64: 2333-2337.
- [16] Su Y, Hu P, Lee SH and Sinko PJ. Using novobioicin as a specific inhibitor of breast cancer resistant protein to assess the role of transporter in the absorption and disposition of topotecan. *J Pharm Pharm Sci* 2007; 10: 519-536.
- [17] Su Y, Lee SH and Sinko PJ. Inhibition of efflux transporter ABCG2/BCRP does not restore mitoxantrone sensitivity in irinotecan-selected human leukemia CPT-K5 cells: evidence for multifactorial multidrug resistance. *Eur J Pharm Sci* 2006; 29: 102-110.
- [18] Yoshikawa M, Ikegami Y, Sano K, Yoshida H, Mitomo H, Sawada S and Ishikawa T. Transport of SN-38 by the wild type of human ABC transporter ABCG2 and its inhibition by quercetin, a

KRAS mutation subtype is a sensitivity biomarker for FL118

- natural flavonoid. *J Exp Ther Oncol* 2004; 4: 25-35.
- [19] Shishido Y, Ueno S, Yamazaki R, Nagaoka M and Matsuzaki T. ABCG2 inhibitor YHO-13351 sensitizes cancer stem/initiating-like side population cells to irinotecan. *Anticancer Res* 2013; 33: 1379-1386.
- [20] Kruijtzter CM, Beijnen JH, Rosing H, ten Bokkel Huinink WW, Schot M, Jewell RC, Paul EM and Schellens JH. Increased oral bioavailability of topotecan in combination with the breast cancer resistance protein and P-glycoprotein inhibitor GF120918. *J Clin Oncol* 2002; 20: 2943-2950.
- [21] de Vries NA, Zhao J, Kroon E, Buckle T, Beijnen JH and van Tellingen O. P-glycoprotein and breast cancer resistance protein: two dominant transporters working together in limiting the brain penetration of topotecan. *Clin Cancer Res* 2007; 13: 6440-6449.
- [22] Takeba Y, Sekine S, Kumai T, Matsumoto N, Nakaya S, Tsuzuki Y, Yanagida Y, Nakano H, Asakura T, Ohtsubo T and Kobayashi S. Irinotecan-induced apoptosis is inhibited by increased P-glycoprotein expression and decreased p53 in human hepatocellular carcinoma cells. *Biol Pharm Bull* 2007; 30: 1400-1406.
- [23] Tagen M, Zhuang Y, Zhang F, Harstead KE, Shen J, Schaiquevich P, Fraga CH, Panetta JC, Waters CM and Stewart CF. P-glycoprotein, but not multidrug resistance protein 4, plays a role in the systemic clearance of irinotecan and SN-38 in mice. *Drug Metab Lett* 2010; 4: 195-201.
- [24] Filipinski E, Berland E, Ozturk N, Guettier C, van der Horst GT, Levi F and Okyar A. Optimization of irinotecan chronotherapy with P-glycoprotein inhibition. *Toxicol Appl Pharmacol* 2014; 274: 471-479.
- [25] Westover D, Ling X, Lam H, Welch J, Jin C, Gongora C, Del Rio M, Wani M and Li F. FL118, a novel camptothecin derivative, is insensitive to ABCG2 expression and shows improved efficacy in comparison with irinotecan in colon and lung cancer models with ABCG2-induced resistance. *Mol Cancer* 2015; 14: 92.
- [26] Zhou L, Weng Q, Zheng Y, Zhou Y, Li Q and Li F. Uptake and efflux of FL118 and two FL118 derivatives in 3D cell model. *Cytotechnology* 2019; 12: 785-795.
- [27] Weng Q, Zhou L, Xia L, Zheng Y, Zhang X, Li F and Li Q. In vitro evaluation of FL118 and 9-Q20 cytotoxicity and cellular uptake in 2D and 3D different cell models. *Cancer Chemother Pharmacol* 2019; 84: 527-537.
- [28] Ling X, Liu XJ, Zhong K, Smith N, Prey J and Li F. FL118, a novel camptothecin analogue, overcomes irinotecan and topotecan resistance in human tumor xenograft models. *Am J Transl Res* 2015; 7: 1765-1781.
- [29] Ling X, Wu W, Fan C, Xu C, Liao J, Rich LJ, Huang RY, Repasky EA, Wang X and Li F. An ABCG2 non-substrate anticancer agent FL118 targets drug-resistant cancer stem-like cells and overcomes treatment resistance of human pancreatic cancer. *J Exp Clin Cancer Res* 2018; 37: 240.
- [30] Zhang D, Wang J, Yang Z, Liu J, Liu Z, Ji L, Liu R, Lin Q and Jiang G. A novel camptothecin analogue FL118 reduces cisplatin resistance of non-small cell lung cancer cells. *Int J Clin Exp Med* 2016; 9: 13501-13513.
- [31] Wang J, Liu Z, Zhang D, Liu R, Lin Q, Liu J, Yang Z, Ma Q, Sun D, Zhou X and Jiang G. FL118, a novel survivin inhibitor, wins the battle against drug-resistant and metastatic lung cancers through inhibition of cancer stem cell-like properties. *Am J Transl Res* 2017; 9: 3676-3686.
- [32] Li F, Ling X and Cao S. Novel formulations of water-insoluble chemical compounds and methods of using a formulation of compound FL118 for cancer therapy (PCT/US2011/058558). USPTO. USA: Roswell Park Cancer Institute; 2011.
- [33] Ling X and Li F. Use of the FL118 core chemical structure platform to generate FL118 derivatives for treatment of human disease (PCT/US2015/022095). USA: 2015.
- [34] Ling X, Li QY and Li F. Matter of composition, synthesis, formulation and application of FL118 platform positions 7 and 9-derived analogues for treatment of human disease (PCT/US19/51595). Canget BioTekpharm, USA and Zhejiang University of Technology, China, 2019.
- [35] Ling X, Bernacki RJ, Brattain MG and Li F. Induction of survivin expression by taxol (paclitaxel) is an early event which is independent on taxol-mediated G2/M arrest. *J Biol Chem* 2004; 279: 15196-15203.
- [36] Ling X, Yang J, Tan D, Ramnath N, Younis T, Bundy BN, Slocum HK, Yang L, Zhou M and Li F. Differential expression of survivin-2B and survivin-DeltaEx3 is inversely associated with disease relapse and patient survival in non-small-cell lung cancer (NSCLC). *Lung Cancer* 2005; 49: 353-361.
- [37] Park MT, Kim MJ, Suh Y, Kim RK, Kim H, Lim EJ, Yoo KC, Lee GH, Kim YH, Hwang SG, Yi JM and Lee SJ. Novel signaling axis for ROS generation during K-Ras-induced cellular transformation. *Cell Death Differ* 2014; 21: 1185-1197.
- [38] Zhao J, Ling X, Cao S, Liu X, Wan S, Jiang T and Li F. Antitumor activity of FL118, a survivin, Mcl-1, XIAP, cIAP2 selective inhibitor, is highly

KRAS mutation subtype is a sensitivity biomarker for FL118

- dependent on its primary structure and steric configuration. *Mol Pharm* 2014; 11: 457-467.
- [39] Santha S, Ling X, Aljahdali IAM, Rasam SS, Wang X, Liao J, Wang J, Fountzilas C, Li Q, Qu J and Li F. Mutant kras as a biomarker plays a favorable role in FL118-induced apoptosis, reactive oxygen species (ROS) production and modulation of survivin, Mcl-1 and XIAP in human bladder cancer. *Cancers (Basel)* 2020; 12: 3413.
- [40] Mueller S, Engleitner T, Maresch R, Zukowska M, Lange S, Kaltenbacher T, Konukiewitz B, Ollinger R, Zwiebel M, Strong A, Yen HY, Banerjee R, Louzada S, Fu B, Seidler B, Gotzfried J, Schuck K, Hassan Z, Arbeiter A, Schonhuber N, Klein S, Veltkamp C, Friedrich M, Rad L, Barenboim M, Ziegenhain C, Hess J, Dovey OM, Eser S, Parekh S, Constantino-Casas F, de la Rosa J, Sierra MI, Fraga M, Mayerle J, Kloppel G, Cadinanos J, Liu P, Vassiliou G, Weichert W, Steiger K, Enard W, Schmid RM, Yang F, Unger K, Schneider G, Varela I, Bradley A, Saur D and Rad R. Evolutionary routes and KRAS dosage define pancreatic cancer phenotypes. *Nature* 2018; 554: 62-68.
- [41] Redston MS, Caldas C, Seymour AB, Hruban RH, da Costa L, Yeo CJ and Kern SE. p53 mutations in pancreatic carcinoma and evidence of common involvement of homocopolymer tracts in DNA microdeletions. *Cancer Res* 1994; 54: 3025-3033.
- [42] Pellegata NS, Sessa F, Renault B, Bonato M, Leone BE, Solcia E and Ranzani GN. K-ras and p53 gene mutations in pancreatic cancer: ductal and nonductal tumors progress through different genetic lesions. *Cancer Res* 1994; 54: 1556-1560.
- [43] Yamaguchi Y, Watanabe H, Yrdiran S, Ohtsubo K, Motoo Y, Okai T and Sawabu N. Detection of mutations of p53 tumor suppressor gene in pancreatic juice and its application to diagnosis of patients with pancreatic cancer: comparison with K-ras mutation. *Clin Cancer Res* 1999; 5: 1147-1153.
- [44] Boutin AT, Liao WT, Wang M, Hwang SS, Karpnits TV, Cheung H, Chu GC, Jiang S, Hu J, Chang K, Vilar E, Song X, Zhang J, Kopetz S, Futreal A, Wang YA, Kwong LN and DePinho RA. Oncogenic Kras drives invasion and maintains metastases in colorectal cancer. *Genes Dev* 2017; 31: 370-382.
- [45] Okamoto K, Zaanani A, Kawakami H, Huang S and Sinicrpe FA. Reversal of mutant KRAS-mediated apoptosis resistance by concurrent Noxa/Bik induction and Bcl-2/Bcl-xL antagonism in colon cancer cells. *Mol Cancer Res* 2015; 13: 659-669.
- [46] Di Bartolomeo M, Pietrantonio F, Perrone F, Dotti KF, Lampis A, Bertan C, Beretta E, Rimasasa L, Carbone C, Biondani P, Passalacqua R, Pilotti S and Bajetta E; Italian Trials in Medical Oncology Group. Lack of KRAS, NRAS, BRAF and TP53 mutations improves outcome of elderly metastatic colorectal cancer patients treated with cetuximab, oxaliplatin and UFT. *Target Oncol* 2014; 9: 155-162.
- [47] Jin HO, Yoon SI, Seo SK, Lee HC, Woo SH, Yoo DH, Lee SJ, Choe TB, An S, Kwon TJ, Kim JI, Park MJ, Hong SI, Park IC and Rhee CH. Synergistic induction of apoptosis by sulindac and arsenic trioxide in human lung cancer A549 cells via reactive oxygen species-dependent down-regulation of survivin. *Biochem Pharmacol* 2006; 72: 1228-1236.